PHILOSOPHICAL TRANSACTIONS OF THE ROYAL SOCIETY A MATHEMATICAL, PHYSICAL & ENGINEERING SCIENCES

Non-stoichiometry and properties of mixed-valence manganites

Alonso J. A.

Phil. Trans. R. Soc. Lond. A 1998 **356**, 1617-1634
doi: 10.1098/rsta.1998.0238

The Royal Society

Non-stoichiometry and properties of mixed-valence manganites

By J. A. Alonso

Instituto de Ciencia de Materiales de Madrid, CSIC Cantoblanco, E-28049 Madrid, Spain

Two families of perovskites, $LaMnO_{3+\delta}$ and $R_{1-x}MnO_{3-\delta}$ (R = La, Pr, Nd) have been prepared in polycrystalline form by a soft-chemistry route. The precursors were annealed at moderate temperatures either in air or under high oxygen pressure. In the strongly oxygenated $LaMnO_{3+\delta}$ perovskites (with nominal Mn^{4+} contents up to 58%), a detailed neutron powder diffraction study shows the presence of both La and Mn vacancies, the Mn being in a substantially higher proportion. The presence of Mn vacancies perturbs the conduction paths for the transport of holes across Mn–O–Mn, weakening the double-exchange interaction. The unwanted presence of Mn vacancies can be minimized in the $R_{1-x}MnO_{3-\delta}$ family: for $x > 0.07$ the insulator–metal transition at temperatures close to T_C is recovered, as well as the colossal magnetoresistance behaviour.

Keywords: neutron diffraction; pressure, high oxygen; defect perovskites; magnetic structures; structure refinement; oxygen excess perovskites

1. Introduction

The structure and properties of the perovskite $LaMnO_3$ and related materials have been extensively studied in the past (Jonker & Van Santen 1950; Wollan & Koeler 1955). More recently, the observation of large negative magnetoresistance effects in mixed-valence manganites (von Helmholt *et al*. 1993) based on $LaMnO_3$ has renewed the interest in the study of these systems (Cheetham *et al*. 1996; Töpfer & Goodenough 1997). In particular, the strongly correlated magnetic and electrical properties are being widely studied. The magnetoresistance is associated with the insulator–metal transition which occurs in the vicinity of the Curie point, for ferromagnetic compositions such as $La_{0.7}Ca_{0.3}MnO_3$, which, thus, simultaneously exhibit metallic conductivity and ferromagnetism at low temperatures. The presence of divalent alkali-earth cations on the La sites of the perovskite induces a Mn^{3+}–Mn^{4+} mixed-valence state with the formation of holes which undergo fast hopping between the two oxidation states. The temperature of both transitions depends on the Mn^{4+} content (for instance, in the $La_{1-x}Ca_xMnO_3$ system T_C varies between 182 and 278 K for Mn^{4+} contents between 14 and 38%, respectively (Rao *et al*. 1996)).

A Mn^{3+}–Mn^{4+} mixed-valence state can also be induced in phases of nominal stoichiometry $LaMnO_{3+\delta}$ (with an Mn^{4+} content of 2δ per formula unit). These phases also show ferromagnetic behaviour for a sufficiently high content of Mn^{4+}. For instance, $LaMnO_{3.08}$ (with 16% of Mn^{4+}) was reported to be ferromagnetic with a Curie temperature $T_C = 125$ K (Hauback *et al*. 1996). Insulator–metal transitions have been described for $LaMnO_{3+\delta}$ for $\delta > 0.12$ (Töpfer *et al*. 1996), and in

$La_{1-x}MnO_3$ for $x \leqslant 0.2$ (Arulraj *et al.* 1996). In fact, GMR behaviour has been reported (Mahendiran *et al.* 1996; Rao & Cheetham 1996) in samples with moderate δ values, showing overall compositions $LaMnO_{3.17}$ and $LaMnO_{3.12}$.

The crystal structure of the oxygen excess rhombohedral phases has been investigated by neutron diffraction (Tofield & Scott 1974; Van Roosmalen *et al.* 1994). Tofield & Scott (1974) and, later on, Van Roosmalen *et al.* (1994) and Van Roosmalen & Cordfunke (1994) concluded that instead of incorporating oxygen interstitials, as directly suggested by the formula $LaMnO_{3+\delta}$, this perovskite is defective in both La and Mn positions: for instance, a sample with a formal composition of $LaMnO_{3.158}$ was found to exhibit an actual crystallographic formula of $La_{0.95}Mn_{0.95}O_3$.

With the aim of studying the influence of the preparative conditions in the structure and properties of bulk mixed-valence manganites, we prepared and characterized two series of compounds: the parent perovskites $LaMnO_{3+\delta}$ (Alonso *et al.* 1996), with a wide range of δ values, $0.11 \leqslant \delta \leqslant 0.31$, and the lanthanide defective $R_{1-x}MnO_3$ (R = La, Pr, Nd) phases. The synthesis was carried out by annealing finely divided precursors at moderate temperatures, either in air or under high oxygen pressure. Structural studies from high resolution neutron diffraction data allowed us to give detailed information about the true defect structures. The influence of the observed defective structures on the physical properties is discussed.

2. Experimental

Two families of samples, $LaMnO_{3+\delta}$ and $R_{1-x}MnO_{3-\delta}$ (R = La, Pr, Nd) have been prepared in polycrystalline form by a sol-gel technique: by dissolving the metal nitrates in citric acid. The citrate solution was evaporated, with formation of a resin which was slowly decomposed at temperatures up to 600 °C. A subsequent treatment in air at 700 °C for 6 h enabled the total elimination of all the organic materials. The black precursor powders were annealed either in air or under 200 bar of oxygen pressure, at moderate temperatures ranging from 700 to 1100 °C. The samples heated in air were either slowly cooled or quenched to room temperature. Hereafter, the annealing conditions of each sample are specified by the temperature (in °C) followed by '/O_2', '/air' or '/q' to indicate treatments performed under 200 bar of O_2, in air with slow cooling (100 °C h^{-1}), or quenched in air to room temperature, respectively.

The final products were characterized by X-ray powder diffraction (XRD, with Cu K_α radiation), thermal analysis, neutron powder diffraction (NPD), magnetic and transport measurements. Both XRD and NPD patterns were analysed by the Rietveld (1969) method, using the FULLPROF program (Rodríguez-Carvajal 1993).

The oxygen contents of the materials were determined by thermal analysis under reducing conditions (in H_2/N_2 flow): the total weight loss corresponding to the complete reduction of the samples to $\frac{1}{2}R_2O_3 + MnO$ at 950 °C enabled a very precise determination of δ, with an estimated error of ± 0.01 oxygens per formula.

3. Results and discussion

(*a*) $LaMnO_{3+\delta}$ *samples*

$LaMnO_{3+\delta}$ phases were obtained as black powders showing XRD patterns characteristic of rhombohedrally distorted monophased perovskites, except for samples

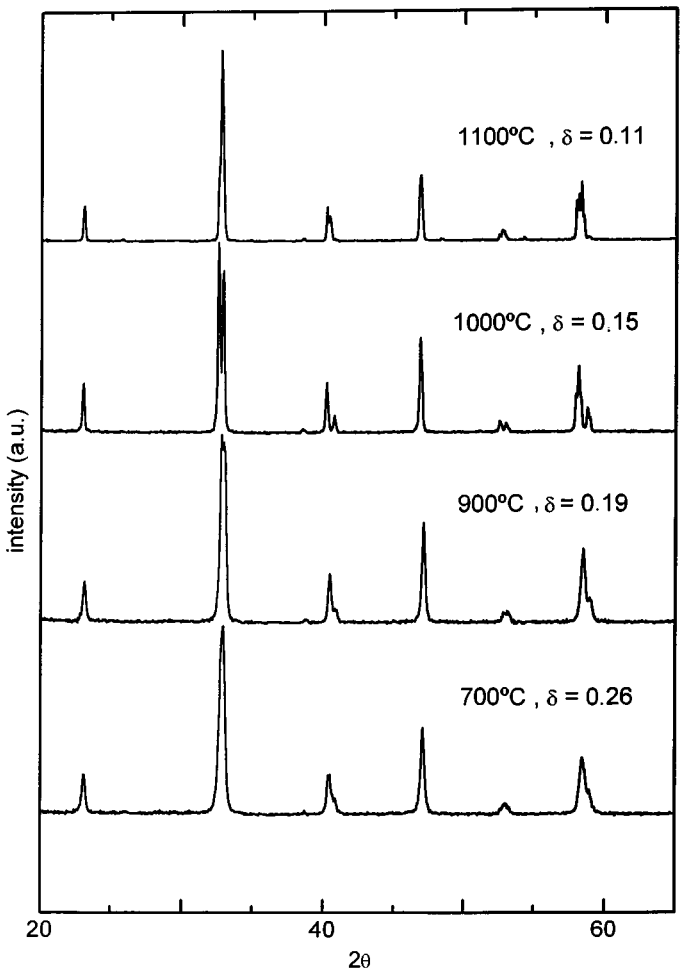

Figure 1. XRD diagrams of $LaMnO_{3+\delta}$ prepared in air (samples A5, A7, A8, A10).

obtained in the less oxidizing conditions, at 1100/air, which showed orthorhombic symmetry. Figure 1 shows the XRD diagrams of some selected samples annealed in air. Observe that there is an increase of the rhombohedral splitting of the peaks as the temperature of the final treatment increases.

The unit-cell parameters of the samples are included in table 1, as well as the values of δ determined by thermal analysis. After the annealings in air, $LaMnO_{3+\delta}$ perovskites showed δ values up to 0.26 (52% Mn^{4+}). The Mn^{4+} content could be increased up to 62% by annealing the samples under 200 bar O_2. Figure 2 shows the unit-cell parameter and volumes per formula (V_f) variation with δ. A net decrease of the rhombohedral angle, α_r, as well as a contraction of the cell dimensions and volume is observed as the oxygen content increases. This effect is correlated with the increasing content of Mn^{4+}, hence increasing the tolerance factor of the perovskite and reducing the rhombohedral distortion of the lattice. For $\delta \leqslant 0.11$, a more distorted orthorhombic stucture is favoured.

The sharp discontinuity in the V_f versus δ variation is striking (figure 2): the

Table 1. *Preparation conditions, unit-cell parameters and volume per formula* (V_f) *for* $LaMnO_{3+\delta}$

(All the samples exhibit rhombohedral symmetry excepting that annealed at 1100/air, orthorhombic.)

sample	preparation conditions	δ	a_h (Å)	c_h (Å)	a_r (Å)	α_r (deg)	V_f (Å^3)
A1	700/O_2	0.31	5.4883(4)	13.311(1)	5.452(1)	60.438(5)	57.87(1)
A2	800/O_2	0.29	5.4898(4)	13.311(1)	5.435(1)	60.450(5)	57.90(1)
A3	900/O_2	0.27	5.4909(4)	13.307(1)	5.452(1)	60.477(5)	57.91(1)
A4	1000/O_2	0.26	5.4951(3)	13.3061(8)	5.453(1)	60.509(5)	57.99(1)
A5	700/air	0.26	5.5097(5)	13.335(2)	5.466(2)	60.53(1)	58.43(2)
A6	800/air	0.22	5.5155(4)	13.338(1)	5.469(1)	60.57(5)	58.56(1)
A7	900/air	0.19	5.5200(3)	13.3335(7)	5.469(1)	60.62(5)	58.64(1)
A8	1000/air	0.15	5.5239(2)	13.3349(7)	5.470(1)	60.64(5)	58.73(1)
A9	1050/air	0.13	5.5350(2)	13.3481(5)	5.478(1)	60.69(5)	59.02(1)
A10	1100/air	0.11	—[a]	—[a]	—	—	59.23(1)

[a]Orthorhombic unit-cell parameters: $a = 5.5400(2)$, 5.4963(2), 7.7876(4) Å.

cell volume suddenly falls from sample A4 to A5, both showing the same oxygen content, $\delta = 0.26$. The samples prepared under high oxygen pressure exhibit an additional contraction with respect to those obtained in air, even showing similar δ values. The subtle differences in their crystal structures are related to the mechanism of incorporation of the excess oxygen. A neutron diffraction study allowed us to determine the nature of those differences.

Four selected samples, A2, A4, A8 and A10, annealed at 800/O_2, 1000/O_2, 1000/air and 1100/air, respectively, were studied in the D2B high resolution neutron diffractometer, at the Institute Laue Langevin, Grenoble, with $\lambda = 1.594$ Å. The room temperature NPD patterns of samples A2, A3 and A8 were refined in the space group $R\bar{3}c$, hexagonal description ($Z = 6$). La atoms are at 6a, $(0, 0, \frac{1}{4})$ positions; Mn at 6b, $(0, 0, 0)$; and O at 18e, $(x, 0, \frac{1}{4})$. Details of the refinement are given elsewhere (Alonso *et al.* 1997*b*). The good matching of the fits is illustrated in figure 3 for sample A2, $LaMnO_{3.29}$. No extra lines or additional splitting of the peaks was observed in any case. The refinement of the occupancy factor of La and Mn led to values significantly lower than 1. For sample A10, the profile refinement was performed in the orthorhombic space group $Pbnm$ ($Z = 4$), according to the $GdFeO_3$ structural model. La is placed at 4c, $(x, y, \frac{1}{4})$; Mn at 4b, $(\frac{1}{2}, 0, 0)$; O1 at 4c and O_2 at 8d, (x, y, z).

Table 2 summarizes the most relevant parameters determined from the refinements. Observe that in the orthorhombic structure (A10) the MnO_6 octahedra do not show any appreciable Jahn–Teller distortion. This result was expected for the relatively high proportion of Mn^{4+} in the crystal (for $\delta = 0.11$, $[Mn^{4+}] = 22\%$), which prevents the cooperative distortion of the octahedra observed (Norby *et al.* 1995) in stoichiometric $LaMnO_{3.00}$.

The crystallographic formulae of the $LaMnO_{3+\delta}$ phases, according to the refined occupancy factors for La and Mn, can be written as $La_{1-x}Mn_{1-y}O_3$, as indicated in table 3. Under more oxidizing conditions (from sample A10 to sample A2) the

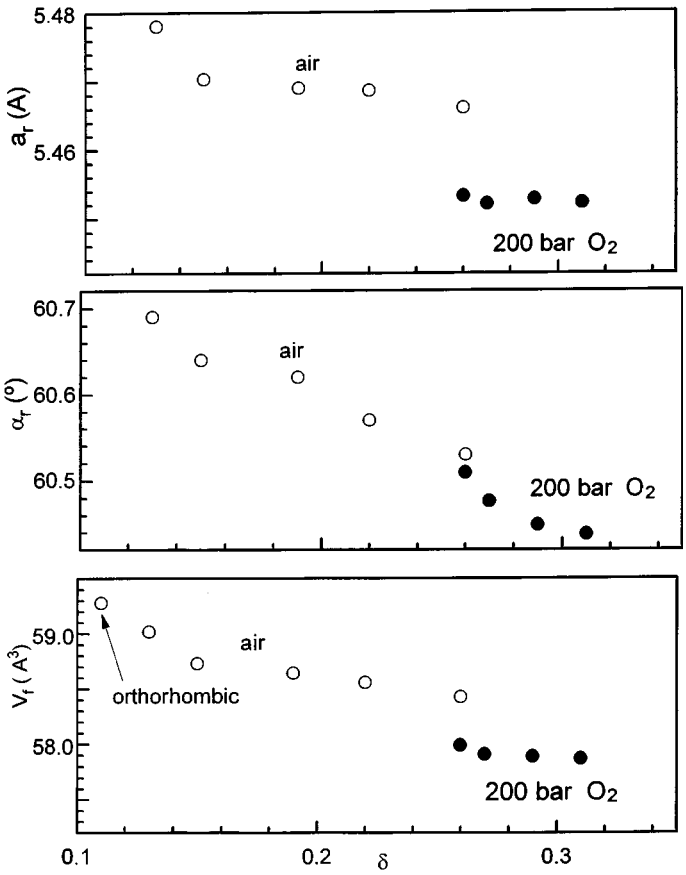

Figure 2. Variation of the unit-cell parameters and volume per formula (V_f) with δ in $LaMnO_{3+\delta}$.

amount of Mn vacancies increases more quickly than the La vacancies, as shown in figure 4. The very oxidizing conditions (under 200 bar O_2) are more easily able to create Mn vacancies than La vacancies. The final valences for Mn calculated from the metal vacancy concentration agree quite well with those determined by thermal analysis, as indicated in table 2. The oxidative non-stoichiometry determined for these products is thus able to explain the macroscopic behaviour, represented by the δ values.

In their pioneering work, Tofield & Scott (1974) and, later on, Van Roosmalen *et al.* (1994) and Van Roosmalen & Cordfunke (1994) concluded that the defect chemistry of $LaMnO_{3+\delta}$ is better described with randomly distributed La and Mn vacancies, present in equal amounts in the solid, in such a way that the crystallographic formula should be written as $La_{1-x}Mn_{1-x}O_3$, with $x = \delta/(3+\delta)$. Our neutron diffraction study on samples with high δ values, prepared at relatively low temperatures from finely divided precursors, confirms the presence of significant amounts of La and Mn vacancies, showing definitively that the concentrations of both kinds of metal vacancies are not equal. Moreover, the concentration of Mn vacancies increases at a higher rate when the annealing conditions of the samples become more oxidizing (i.e.

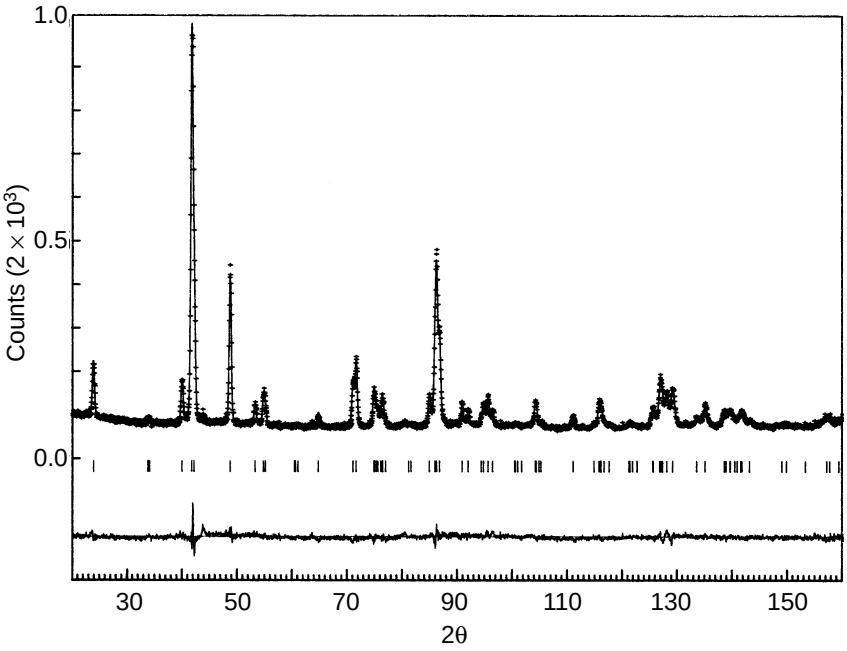

Figure 3. Room temperature observed (crosses), calculated (solid line) and difference (at the bottom) NPD profiles for rhombohedral $LaMnO_{3.29}$, A2.

lower temperatures and higher oxygen pressure), as shown in figure 4. The La and Mn vacancy concentrations only become closer for low δ values, i.e. for samples annealed in air at higher temperatures. Note that the samples described by Tofield & Scott (1974), Van Roosmalen *et al*. (1994) and Van Roosmalen & Cordfunke (1994) had undergone thermal treatments at even higher temperatures of 1200 °C or 1300 °C, respectively.

We show that the non-stoichiometry of $LaMnO_3$ cannot be simply denoted by a single parameter, δ or x, but requires the specification of two parameters, x and y in $La_{1-x}Mn_{1-y}O_3$. The relative values of x and y depend dramatically on the preparation procedures of the samples, in such a way that ceramic synthesis at higher temperatures favours equal values of x and y. The discontinuous variation of V_f versus δ observed for $\delta = 0.26$ in figure 2 is due to the sudden increase in the concentration of Mn vacancies in sample A4, prepared under high O_2 pressure.

The evolution of the neutron diffraction patterns of $LaMnO_{3+\delta}$ as a function of temperature was studied for samples A4, A8 and A10 in the DN5 diffractometer at the Siloé reactor of the CEN-Grenoble, with $\lambda = 2.48$ Å, and it is shown in figure 5. A magnetic contribution on the peaks of nuclear origin can be observed in all the studied samples, corresponding to their three-dimensional magnetic ordering (Alonso *et al*. 1997*a*). There is no magnetic contribution outside the Bragg positions given by the chemical cell, although a very small but significant contribution in peaks forbidden by the space group $R\bar{3}c$ (sample A8), for instance (1 0 1), (0 0 3), indicates a canted structure for the rhombohedral phases. All the magnetic structures can be described in terms of a single propagation vector, $\boldsymbol{k} = (0, 0, 0)$.

The magnetic structure of rhombohedral $LaMnO_{3.15}$ (A8) is shown in figure 6,

Table 2. *Metal occupancy factors,* Mn *valence (from* f_{occ} *and from the thermal analysis* δ *values), main* Mn–O *and* La–O *distances and angles and tolerance factors determined from NPD data at room temperature*

sample	A10	A8	A4	A2
preparation conditions	1100/air	1000/air	1000/O_2	800/O_2
f_{occ}(La)	0.978(2)	0.969(9)	0.97(1)	0.95(1)
f_{occ}(Mn)	0.946(4)	0.927(15)	0.87(2)	0.89(1)
val(Mn)(f_{occ})	3.24	3.33	3.55	3.54
(TG)	0.11	0.15	0.26	0.29
val(Mn)(TG)	3.22	3.30	3.52	3.58
Mn–O (Å)	1.9789(6) 1.975(2) 1.974(2)	1.9634(6)	1.9514(7)	1.9494(6)
⟨O-Mn–O⟩ (deg)	91.52(6)	91.13(5)	90.91(6)	90.84(6)
⟨Mn–O–Mn⟩ (deg)	161.49(1)	163.477(7)	165.264(7)	165.782(7)
⟨La–O⟩ (Å)	2.653(1)	2.659(1)	2.658(1)	2.659(1)
t[a]	0.949	0.958	0.963	0.965

[a]The tolerance factor is defined as $t = \langle \text{La–O} \rangle / \sqrt{2} \langle \text{Mn–O} \rangle$.

Table 3. *Crystallographic formulae determined from the occupancy factors of* La *and* Mn *in* $LaMnO_{3+\delta}$

sample	nominal composition	actual stoichiometry
A2	$LaMnO_{3.29}$	$La_{0.95(1)}Mn_{0.89(1)}O_3$
A4	$LaMnO_{3.26}$	$La_{0.97(1)}Mn_{0.87(2)}O_3$
A8	$LaMnO_{3.15}$	$La_{0.97(1)}Mn_{0.93(1)}O_3$
A10	$LaMnO_{3.11}$	$La_{0.978(2)}Mn_{0.946(4)}O_3$

together with the low temperature NPD profiles after the refinement, including the magnetic contribution to the scattering. The magnetic moments of Mn at $(0, 0, 0)$ and $(0, 0, \frac{1}{2})$ and symmetry-related positions define a canted ferromagnetic structure, constituted by ferromagnetic planes normal to the c-axis, in which the direction of the Mn moments alternates between $[0\,1\,0]$ and $[-1\,1\,0]$ in successive planes. The refined magnitude of Mn magnetic moments at 2 K is 2.5(1) μ_B, and the canting angle is 27(8)°. For orthorhombic $LaMnO_{3.11}$ (A10), the low-temperature ferromagnetic structure is collinear, with the spins of Mn cations ferromagnetically coupled along the c-axis. The refined value of the ordered magnetic moment for Mn cations at 2 K is 3.93(6) μ_B.

The thermal evolution of the ordered magnetic moments of samples A4, A8 and A10 was studied from the NPD patterns collected as a function of temperature. The thermal variation of the magnetic moments is shown in figure 7. The three-dimensional magnetic ordering begins to develop below T_C temperatures (±10 K) of 165 K, 140 K and 65 K for samples A10, A8 and A4, respectively. The ordered magnetic moments gradually increase to reach their maximum value at temperatures close to 2 K. The saturation value of the moments decreases dramatically from A8

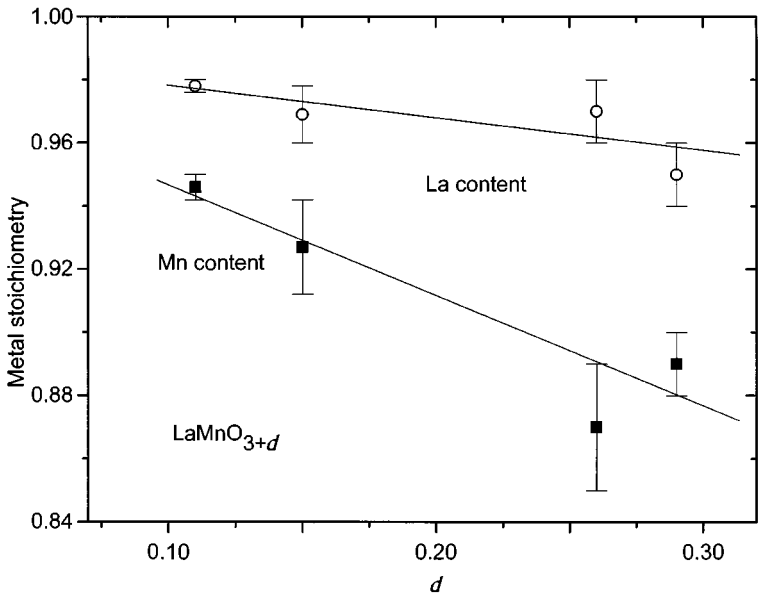

Figure 4. Variation of the La and Mn contents with δ, determined from the neutron diffraction refinements. The full lines are guides for the eye.

to A4 due to competition between ferromagnetic and antiferromagnetic (F and AF) interactions (Töpfer & Goodenough 1997).

The T_C determined by neutron diffraction are plotted versus δ in figure 8. The figure also includes the Curie temperatures obtained from magnetic susceptibility measurements for a more complete set of samples (de Silva *et al*. 1998). T_C values obtained by NPD are systematically lower than those determined from the magnetization curves, as a consequence of a gradual transition from short-range to long-range magnetic order, the last one taking place at temperatures about 5–15 K lower.

Figure 8 shows that T_C decreases as δ increases, i.e. as the Mn^{4+} concentration increases. This behaviour can be interpreted as a consequence of the presence of metal vacancies (see table 2) in the structure. Even if the tolerance factors (table 2) of the perovskite structures of samples A10 to A2 increase with δ, implying more open Mn–O–Mn angles which would favour the double-exchange interaction (Fontcuberta *et al*. 1996; Rao *et al*. 1997), the relatively high proportion of Mn vacancies (e.g. 7% in A8 and 13% in A4) perturbs the connecting paths for the transport of holes across Mn–O–Mn, and makes the ferromagnetic couplings weaker. Also, the presence of random vacancies has an strong localizing effect on the available charges, which perturbs their transport across the crystal (Ranno *et al*. 1996). For very high doping levels such as that exhibited by A4 ($\delta = 0.26$, 52% MnIV) the number of AF couplings severely compete with F interactions, giving rise to frustrated low T_C systems with spin-glass features.

The transport properties, studied in sintered pellets annealed under the same conditions described in table 1, show a semiconducting behaviour in the temperature range 77–300 K for all the studied samples. Figure 9 illustrates the $\ln(R)$ versus $T^{1/4}$ plot for $LaMnO_{3.15}$ (A8), with a nominal Mn^{4+} content of 30%, very close to the

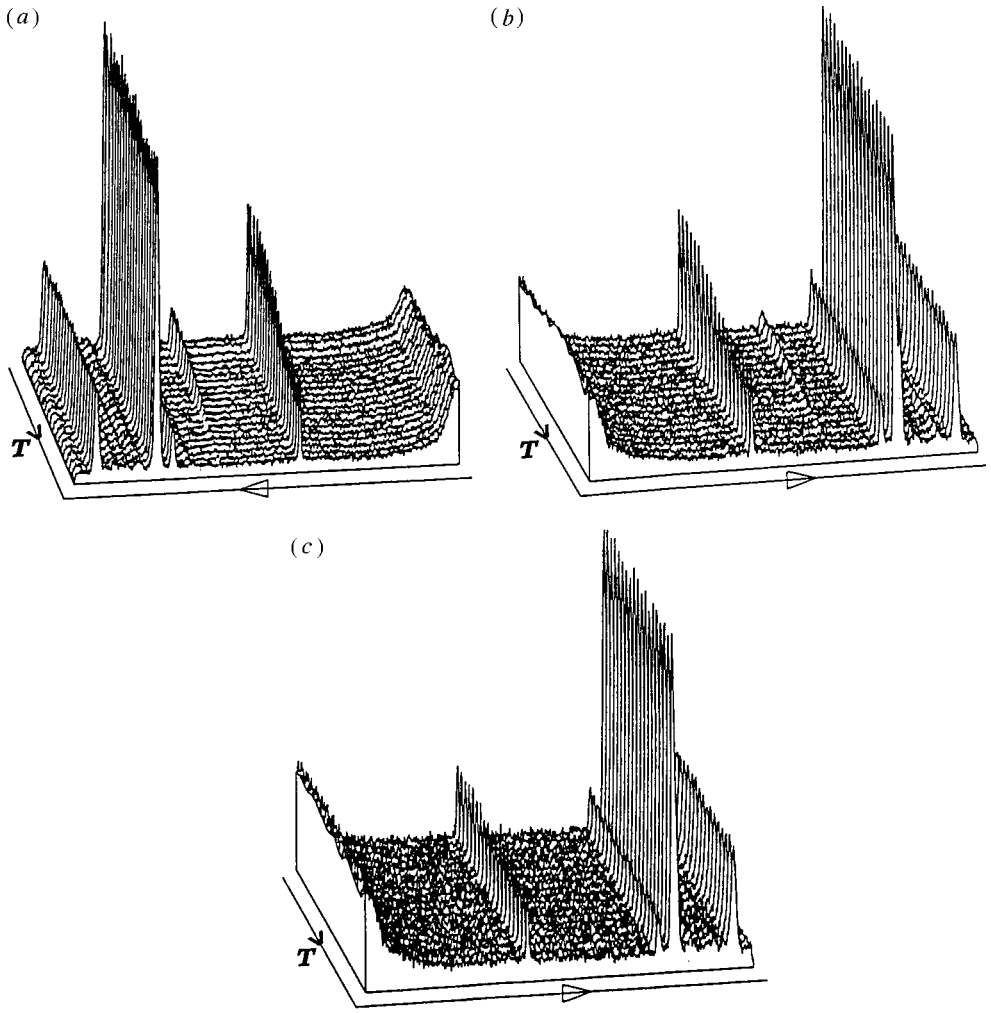

Figure 5. Thermal evolution of the NPD patterns for (*a*) $LaMnO_{3.11}$, A10; (*b*) $LaMnO_{3.15}$, A8; (*c*) $LaMnO_{3.26}$, A4. Below T_C, the magnetic contribution on the peaks of nuclear origin corresponds to the three-dimensional ferromagnetic ordering.

'optimum' value of 33% (Rao *et al*. 1996). A variable range hopping mechanism is observed between 77 and 300 K, with no insulator–metal transition below temperatures close to T_C (for A8, $T_C = 140$ K).

The high concentration of defects, observed by neutron diffraction, mostly in the Mn sublattice, is believed to be in the origin of the anomalous magnetic and transport properties: the samples are ferromagnetic below T_C which decreases when δ increases, even if t increases; all the samples are semiconducting, showing no metallic regime below T_C. The preparation by soft-chemistry methods of $LaMnO_{3+\delta}$ materials with high δ contents starting from La:Mn = 1:1 mixtures leads to highly Mn-defective phases with anomalous electrical and magnetic properties. In order to achieve the synthesis of undoped La–Mn–O materials with a perfect Mn sublattice, it was necessary to start from mixtures with La:Mn < 1 ratios, in such a way that the selective

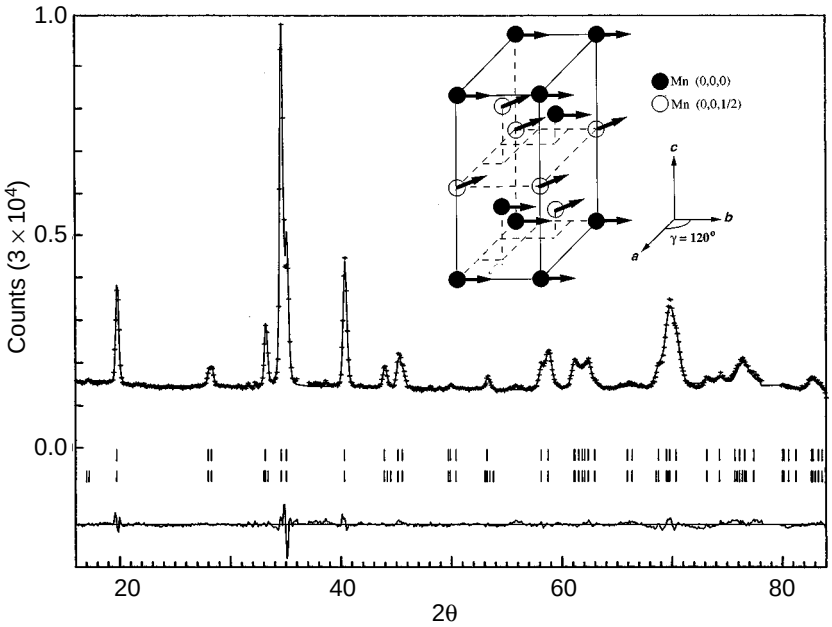

Figure 6. NPD profiles for rhombohedral $LaMnO_{3.15}$, collected at 2 K. The magnetic contribution to the scattering is included. The inset shows the canted magnetic structure at 2 K.

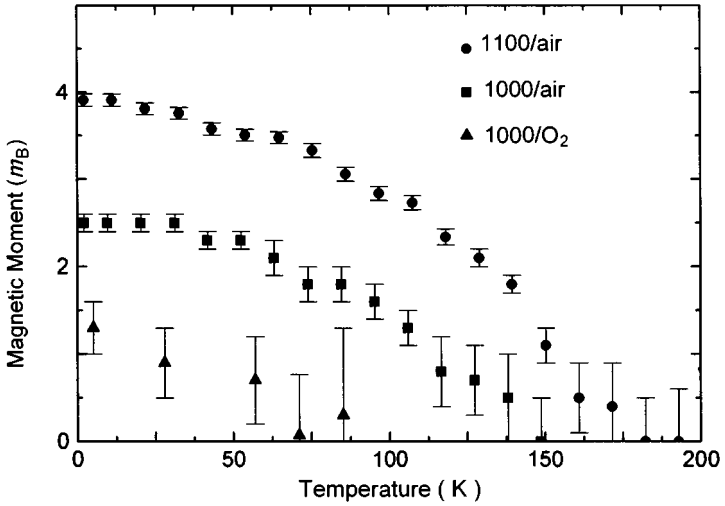

Figure 7. Thermal evolution of the ordered magnetic moments for $LaMnO_{3.11}$, $LaMnO_{3.15}$, $LaMnO_{3.16}$, determined by NPD.

creation of La vacancies allows Mn cations to reach the valence corresponding to the oxidation potential given by the preparative conditions.

(*b*) $La_{1-x}MnO_{3-\delta}$ *samples*

The compounds of the series $La_{1-x}MnO_{3-\delta}$ ($x = 0.07, 0.11, 0.17, 0.33$), as well as the materials of nominal stoichiometry, $R_{0.89}MnO_{3-\delta}$ (R = Pr, Nd), were prepared

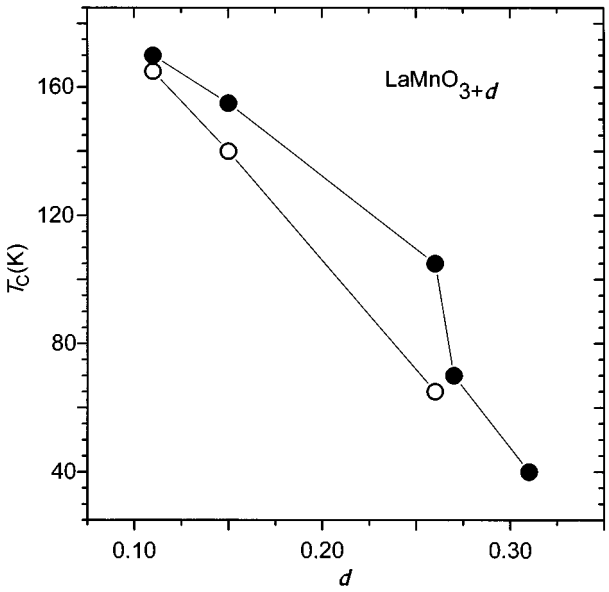

Figure 8. Variation of the Curie temperature with δ. Full symbols from magnetization data, open symbols from NPD data.

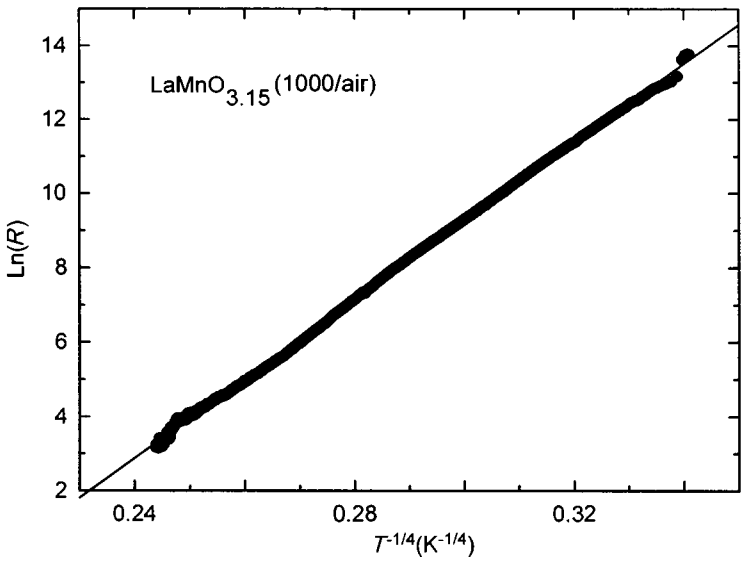

Figure 9. Variation of the electrical resistance with temperature, in a $\ln(R)$ versus $T^{1/4}$ plot.

from citrate precursors, decomposed and annealed under three different conditions: 1000/q, 1000/air and 800/O_2. Monophased perovskites were identified in the final products by XRD, except for the most La-deficient samples ($x = 0.33$) annealed in air or quenched, in which Mn_3O_4 impurities were detected, as shown in figure 10. After annealing under 200 bar O_2, pure perovskite phases were obtained. Table 4 lists the unit-cell parameters of the perovskites determined by XRD. As a general

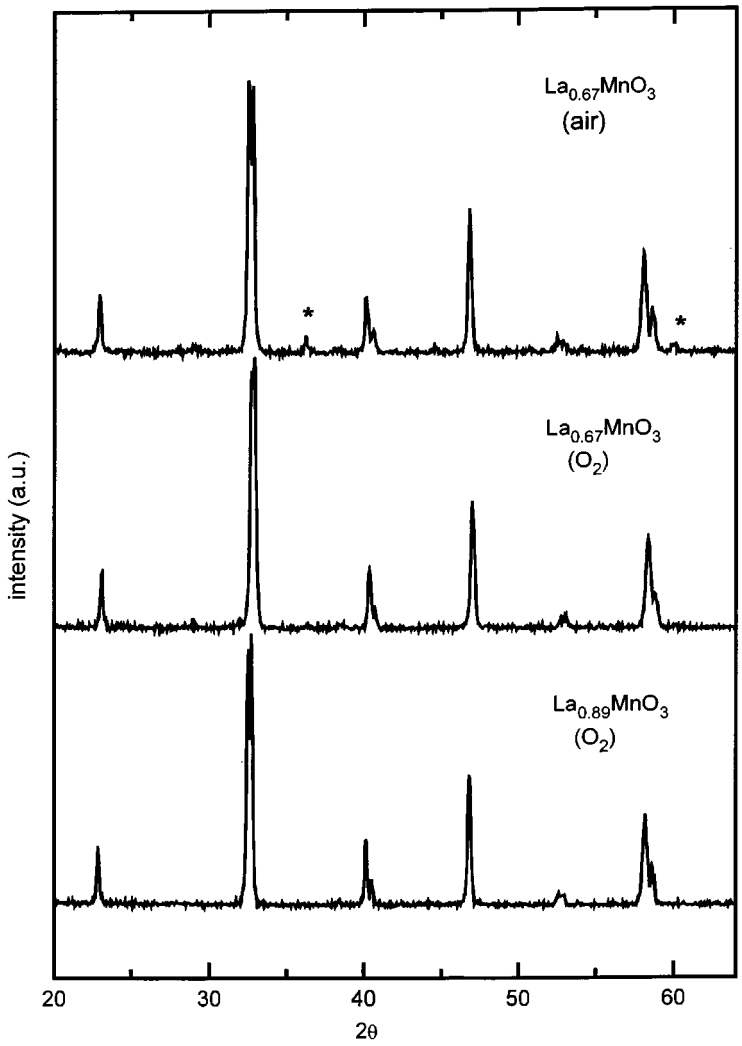

Figure 10. XRD diagrams of $La_{0.67}MnO_3$ annealed either in air or in high O_2 pressure. The diagram of $La_{0.89}MnO_3$ is given for comparative purposes. The stars ($\star$) correspond to the most intense reflections of Mn_3O_4.

rule, the perovskite distortion decreases in samples prepared under more oxidizing conditions.

Some selected samples were studied by high-resolution NPD. In table 5 the most relevant parameters after the profile refinement of the patterns are included. For the La perovskites, the first important result is that all the studied samples show a defective O sublattice, even for the smallest La deficiency, of $x = 0.07$. For a given La content (e.g. $x = 0.11$), the more oxidizing are the annealing conditions, the more complete is the oxygen sublattice, and the more regular is the perovskite structure: the tolerance t factors increase and the Mn–O–Mn angles become more open. The Mn occupancy factors were normalized to unity during the refinements. However, density measurements show that some Mn vacancies are still present in slightly La-deficient

Table 4. *Preparation conditions, crystal data and ferromagnetic* T_C *(in* K*) of* $R_{1-x}MnO_3$ (R = La, Pr, Nd) *perovskites*

(Unit-cell dimensions are given in Å, V in Å^3.)

condition		$La_{0.93}$	$La_{0.89}$	$La_{0.83}$	$La_{0.67}$	$Pr_{0.89}$	$Nd_{0.89}$
1000/q	a	5.5408(8)	5.5422(5)	5.5391(5)	—	5.4686(7)	5.4159(6)
	b	5.5025(8)				5.5904(7)	5.7198(6)
	c	7.800(1)	13.397(1)	13.380(1)		7.670(1)	7.5965(8)
	V	237.81	355.89	355.53		234.48	235.33
	T_C	151.3	189.3	223.2		82.8	72.9
1000/air	a	5.5294(6)	5.5304(6)	5.5260(4)	5.5238(4)	—	—
	c	13.389(1)	13.360(2)	13.357(1)	13.364(1)		
	V	353.47	353.89	353.26	353.15		
	T_C	112.1	195.0	237.7	255.0		
800/O_2	a	5.4889(4)	5.5019(4)	5.5043(5)	5.5012(5)	5.5027(5)	—
	c	13.311(1)	13.320(1)	13.334(1)	13.326(1)	13.344(2)	
	V	347.40	349.20	349.85	349.27	349.94	
	T_C	54.3	142.1	163.7	134.8	—	

Table 5. *Relevant parameters after the refinement of NPD data, at* 295 K*, of* $R_{1-x}MnO_3$ *perovskites annealed at different conditions*

(Bond distances are given in Å, angles in degrees.)

R_{1-x} AC[a]	$La_{0.93}$ 800/O_2	$La_{0.89}$ 1000/q	$La_{0.89}$ 1000/air	$La_{0.89}$ 800/O_2	$La_{0.83}$ 800/O_2	$Pr_{0.89}$ 800/O_2
f_{occ}(La)	0.91(1)	0.87(1)	0.882(9)	0.87(1)	0.870(9)	0.890(8)
f_{occ}(Mn)	1.00	1.00	1.00	1.00	1.00	0.97(1)
f_{occ}(O)	2.98(3)	2.85(3)	2.89(3)	2.90(3)	2.91(3)	3.00
Mn–O	1.953(4)	1.969(4)	1.964(4)	1.952(4)	1.953(4)	1.9593(8) 1.960(3) 1.963(3)
Mn–O–Mn	164.97(1)	162.98(1)	163.62(5)	165.40(1)	165.57(1)	158.17 158.74
⟨La–O⟩	2.656(4)	2.663(4)	2.661(4)	2.660(4)	2.663(4)	2.562(4)
t	0.962	0.956	0.958	0.964	0.964	0.924

[a]AC, annealing conditions.
[b]$t = \langle La–O\rangle/\sqrt{2}\langle Mn–O\rangle$.

samples, and the concentration of Mn vacancies very quickly decreases as x increases. When starting from nominal La-defective compositions there is a dramatic impact on the Mn sublattice, as expected. For $Pr_{0.89}MnO_3$ the absence of distortion in the MnO_6 octahedra is striking in the sample annealed under high O_2 pressure, due to the vanishing of the cooperative Jahn–Teller effect, for a nominal Mn^{4+} concentration of 33%.

All the samples studied show a ferromagnetic behaviour; the T_C values are included

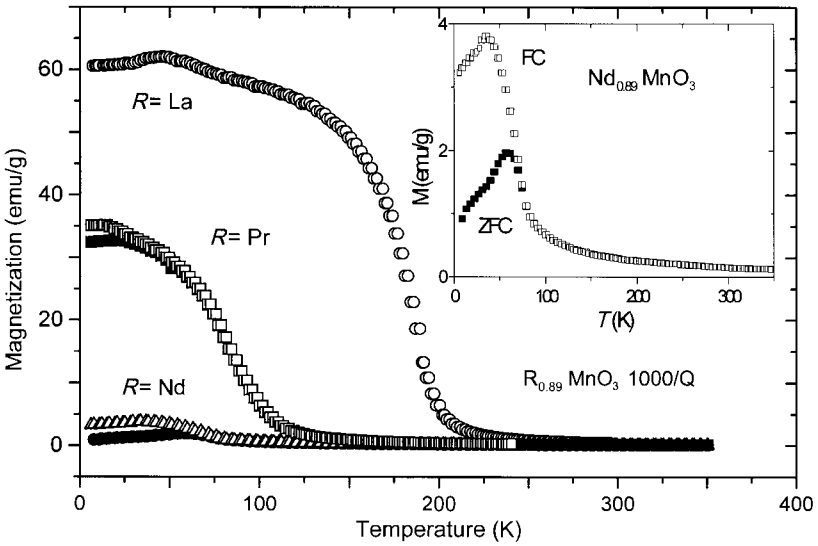

Figure 11. Magnetization versus temperature plot for $R_{0.89}MnO_3$ (R = La, Pr, Nd), prepared at 1000/q.

in table 5. As a general rule, for increasing x values T_C increases as a consequence of the increment in the Mn^{4+} concentration and the progressive opening of the Mn–O–Mn angles, controlling the transfer integral between Mn^{3+}–O–Mn^{4+}. Figure 11 illustrates this effect for the family of samples $R_{0.89}MnO_3$ (R = La, Pr, Nd), in which the tolerance factor ranges from 0.956 ($T_C = 189.3$ K, R = La) to 0.916 ($T_C = 72.9$, R = Nd). In the severely distorted perovskites for R = Pr, Nd, the observation of irreversibilities at low temperatures suggests the presence of clustering effects, which are currently under study.

The transport properties show a semiconducting-like behaviour for the samples annealed in air or followed by quenching. Only for the compounds annealed under high oxygen pressure is the metallic behaviour recovered, showing insulator–metal transitions, as illustrated in figure 12*a* for $La_{0.89}MnO_3$. Of the samples annealed in O_2, only those with the lowest La deficiency ($x = 0.07$) are semiconducting over all the temperature range, as shown in figure 12*b*. The samples with $x = 0.11$, 0.17, 0.33 show magnetoresistive behaviour, with colossal magnetoresistance amplitudes of 30–40% at $H = 1$ T.

4. Conclusions

In § 3 *a* we proposed that the anomalous transport and magnetic properties observed in $LaMnO_{3+\delta}$ samples prepared by soft-chemistry procedures, including annealings at moderate temperatures, could be explained by the unwanted presence of metal vacancies in the Mn sublattice. These Mn vacancies could be minimized by suitably introducing metal vacancies in the La sublattice, as shown in § 3 *b*. High oxygen pressure, which leads to highly Mn-defective materials when starting from stoichiometric $LaMnO_3$ precursors, is, however, a useful tool when preparing La-defective perovskites, since it helps to complete the oxygen sublattice, and to recover the metallic regime below the insulator–metal transition. Unwanted Mn vacancies can also be

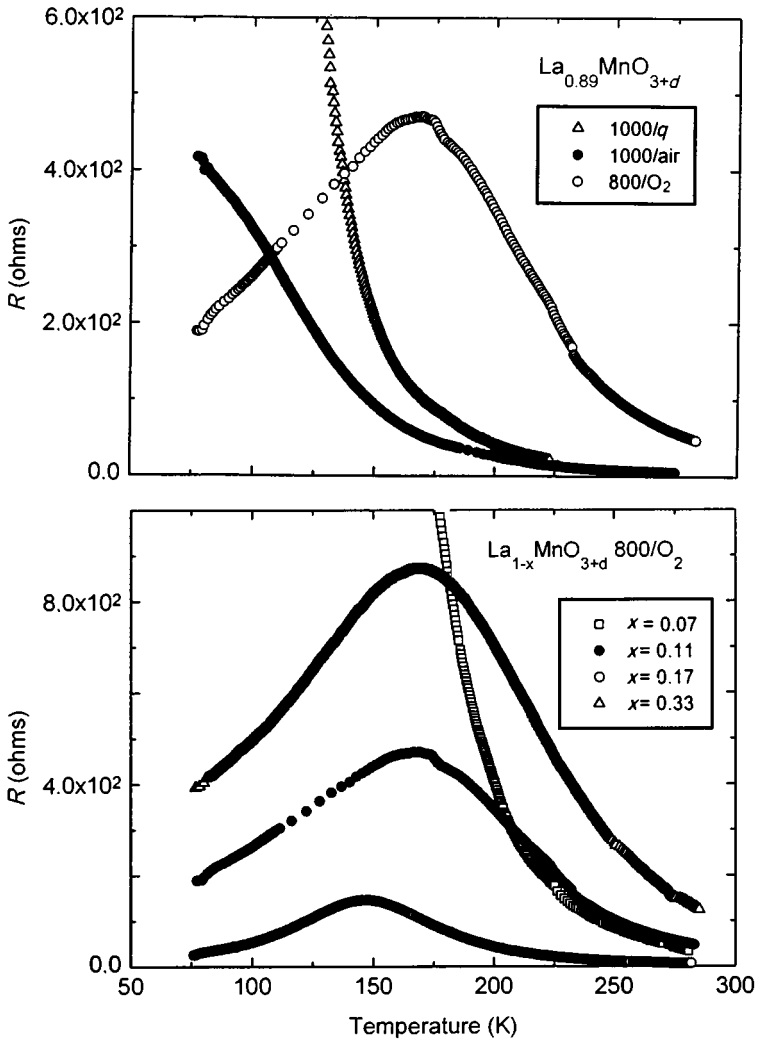

Figure 12. Electrical resistance versus temperature plot for (*a*) $La_{0.89}MnO_3$, annealed at different conditions (*b*) $La_{1-x}MnO_3$ annealed in high O_2 pressure.

present in alkaline-earth-doped perovskites, when annealing in oxidizing conditions. This fact must be taken into account when determining the preparation conditions of colossal magnetoresistance materials with optimized properties.

This work has been done in collaboration with M. J. Martínez-Lope and M. T. Casais of the Instituto de Ciencia de Materiales de Madrid; J. L. García-Muñoz of the Instituto de Ciencia de Materiales de Barcelona; J. L. MacManus-Driscoll, L. F. Cohen and S. de Silva at Imperial College, London.

References

Alonso, J. A., Martínez-Lope, M. J. & Casais, M. T. 1996 *Eur. J. Solid State Inorg. Chem.* **33**, 331.

Alonso, J. A., Martínez-Lope, M. J., Casais, M. T. & Muñoz, A. 1997*a* *Solid State Commun.* **102**, 7.

Alonso, J. A., Martínez-Lope, M. J., Casais, M. T., MacManus-Driscoll, J. L., de Silva, P. S. I. P. N., Cohen, L. F. & Fernández-Díaz, M. T. 1997*b* *J. Mater. Chem.* **7**, 2139.

Arulraj, A., Mahesh, R., Subbanna, G. N., Mahendiran, R., Raychaudhuri, A. K. & Rao, C. N. R. 1996 *J. Solid State Chem.* **127**, 87.

Cheetham, A. K., Rao, C. N. R. & Vogt, T. 1996 *J. Solid State Chem.* **126**, 337.

de Silva, P. S. I. P. N., Richards, F. M., Cohen, L. F., Alonso, J. A., Martínez-Lope, M. J., Casais, M. T., Kodenkandath, T. & MacManus-Driscoll, J. L. 1998 *J. Appl. Phys.* **83**, 394.

Fontcuberta, J., Martínez, B., Seffar, A., Piñol, S., García-Muñoz, J. L. & Obradors, X. 1996 *Phys. Rev. Lett.* **76**, 1122.

Hauback, B. C., Fjellvag, H. & Sakai, N. 1996 *J. Solid State Chem.* **124**, 43.

Jonker, G. H. & Van Santen, J. H. 1950 *Physica* **16**, 337.

Mahendiran, R., Tiwary, S. K., Raychadhuri, A. K., Ramakrisnan, T. V., Mahesh, R., Ragan-vittal, N. & Rao, C. N. R. 1996 *Phys. Rev.* B **53**, 3348.

Norby, P., Andersen, I. G. K., Andersen, E. K. & Andersen, N. H. 1995 *J. Solid State Chem.* **119**, 191.

Ranno, L., Viret, M., Mari, A., Thomas, R. M. & Coey, J. M. D. 1996 *J. Phys. Condens. Matter* **8**, L33.

Rao, C. N. R. & Cheetham, A. K. 1996 *Science* **272**, 369.

Rao, G. H., Sun, J. R., Sun, Y. Z., Zhang, Y. L. & Liang, J. K. 1996 *J. Phys. Condens. Matter* **8**, 5393.

Rao, G. H., Sun, J. R., Liang, J. K. & Zhou, W. Y. 1997 *Phys. Rev.* B **55**, 3742.

Rietveld, H. M. 1969 *J. Appl. Crystallogr.* **2**, 65.

Rodríguez-Carvajal, J. 1993 *Physica* B **192**, 55.

Tofield, B. C. & Scott, W. R. 1974 *J. Solid State Chem.* **10**, 183.

Töpfer, J. & Goodenough, J. B. 1997 *J. Solid State Chem.* **130**, 117.

Töpfer, J., Doumerc, J. P. & Grenier, J. C. 1996 *J. Mater. Chem.* **6**, 1511.

Van Roosmalen, J. A. M. & Cordfunke, E. H. P. 1994 *J. Solid State Chem.* **110**, 106.

Van Roosmalen, J. A. M., Cordfunke, E. H. P., Helmholdt, R. B. & Zandbergen, H. W. 1994 *J. Solid State Chem.* **110**, 100.

von Helmholt, R., Wecker, J., Holzapfel, B., Schultz, L. & Samwer, K. 1993 *Phys. Rev. Lett.* **71**, 2331.

Wollan, E. O. & Koeler, W. C. 1955 *Phys. Rev.* **100**, 545.

Discussion

D. Khomskii (*University of Groningen, The Netherlands*). If samples are prepared nominally stoichiometric LaMn concentration, it is stressed from the very beginning that the oxygen sublattice is always full, but is it ever possible to get real oxygen vacancies, i.e. $LaMnO_{3-\delta}$, so that we have not Mn^{3+}/Mn^{4+} but rather Mn^{2+}/Mn^{3+}?

J. A. Alonso. No, we have never observed this behaviour, either by TG or thermal analysis measurements. We always observed $\delta > 1$, and at the same time neutron diffraction refinements showed that the oxygen lattice is complete. To obtain the sort of samples that Dr Khomskii is talking about, we should work in reducing conditions.

D. Khomskii. In the magnetic structures with the first ferromagnetic layer and the next layer tilted by 30°, is this really a spiral phase in the third direction, or is it that in neutrons you see both ferromagnetic and antiferromagnetic reflections?

J. A. Alonso. No, you only have the same orientation of the moments with the crystallographic axis. So, it is not a spiral structure but a canted structure: the first angle is 0°, then 30°, then 0° again.

J. M. D. Coey (*Trinity College, Dublin, Ireland*). There are reports in the literature that when the manganites are prepared under extremely low oxygen partial pressures, materials which are oxygen deficient, but stoichiometric at the same time, can be obtained.

G. A. Gehring (*University of Sheffield, UK*). Could Dr Alonso clarify the phase diagram (figure 8) that he obtained, because he was implying that when the number of manganese vacancies became very large, T_C and the magnetization dropped. I thought that if you have a stoichiometric material, where you actually have $LaMnO_3$, it should be antiferromagnetic, and that has zero Mn vacancies. So does this mean there is an optimum number of Mn vacancies, which gives you a maximum in T_C when you move from the antiferromagnetic to the ferromagnetic phase, and then more Mn vacancies actually gives you a reduction again?

J. A. Alonso. Yes, it is exactly as you say.

M. Blamire (*University of Cambridge, UK*). How homogeneous are Dr Alonso's materials? In other words, what length-scale determines the homogeneity of the material? He is dealing with materials with vacancies and defects, and clearly for transport measurements the homogeneity is important, but is that not also true for magnetization measurements? His susceptibility measurements could just be due to a range of T_C within the material. Is that possible?

J. A. Alonso. About the homogeneity of the samples: we have observed from the broadening of the reflections that we have a coherence length of the order of 1000 μm. Concerning the possible phase segregation observed by scanning microscopy, we didn't observe any phase segregation by EDX analysis in different parts of the material we always found the same stoichiometry.

M. Blamire. In the non-ferromagnetic state, it is clear that the electrons are sampling rather small distances which are probably at a smaller length-scale than EDX is easily able to probe. Would that have any relevance?

J. A. Alonso. Yes, I agree.

S.-W. Cheong (*Bell Laboratories/Lucent Technologies, USA*). To go back to Dr Khomskii's question about Mn^{2+}, we worked hard to produce Mn^{2+} in a perovskite structure by using oxygen deficiency or putting Ce^{4+} on to the La site, and we found it was very difficult to produce Mn^{2+}. I think the ion is just too large to go into a perovskite structure.

P. C. Riedi (*University of St Andrews, UK*). There is a pretty infallible check for Mn^{2+}: do the NMR in the ferromagnetic state, using Mn^{55}. The Mn^{2+} come in above 600 MHz, whereas the Mn^{3+} and the Mn^{4+} are at 420 MHz and 300 MHz, respectively. In fact, we have seen this in some samples. The Mn^{3+} and Mn^{4+} lines collapse to a single line near 380 MHz for fast electron hopping.

N. D. Mathur (*University of Cambridge, UK*). What reducing conditions would produce a perfect lattice with no vacancies and therefore an insulator?

J. A. Alonso. Just by annealing the samples in an inert atmosphere or under reducing conditions, when you should have just Mn^{3+}.

N. D. Mathur. So if you anneal in 1 atm Ar, you should have a perfect insulator?

J. A. Alonso. Yes.

D. M. Edwards (*Imperial College, London, UK*). In the La-deficient material, Dr Alonso says he gets a more or less perfect Mn sublattice, but it is metallic. What is the carrier concentration? How does it compare with x in the doped LaSr material?

J. A. Alonso. I think it is approximately three times that found in conventional alkaline-earth-doped materials. Holes are introduced by just taking out some La cations, and approximately three times the number of carriers results.

J. P. Attfield (*University of Cambridge, UK*). Returning to the question of Mn^{2+}, we have shown that reduced perovskite $YBaMn_2O_5$, which is exactly 50:50 Mn^{2+} and Mn^{3+}, can be made. It does require reducing conditions and it has a well-defined oxygen defect superstructure. It seems likely that in the sort of slightly reduced samples which Professor Coey has mentioned small amounts of intergrowth of this kind of phase are responsible for the apparent Mn^{2+} content.

P. Battle (*University of Oxford, UK*). Is Dr Alonso confident that the stoichiometry of MnO is sufficiently well-defined to use it as an end-point in a TGA analysis?

J. A. Alonso. I have contrasted it with chemical titrations and have always observed a higher reproducibility by thermal analysis. In compounds in which I am sure about the δ content (for instance, the stoichiometric $LaMnO_3$), the final values from the TG weight loss are exactly what we expect. So yes, I am confident.

PHILOSOPHICAL TRANSACTIONS OF THE ROYAL SOCIETY A MATHEMATICAL, PHYSICAL & ENGINEERING SCIENCES